



Contents lists available at ScienceDirect

Materials Letters

journal homepage: www.elsevier.com/locate/matletNanoscale color control of TiO₂ films with embedded Au nanoparticlesM. Torrell^{a,*}, L. Cunha^a, Md. R. Kabir^{a,b}, A. Cavaleiro^b, M.I. Vasilevskiy^a, F. Vaz^a^a Universidade do Minho, Centro de Física, 4710-057 Braga, Portugal^b SEC-CEMUC – Universidade de Coimbra, Dept. Eng. Mecânica, Pólo II, 3030-788 Coimbra, Portugal

ARTICLE INFO

Article history:

Received 1 July 2010

Accepted 9 August 2010

Available online xxxx

ABSTRACT

We demonstrate an efficient nanoscale control of the optical properties of TiO₂ films by tuning the Surface Plasmon Resonance (SPR) in the embedded Au nanoparticles. The films were grown by reactive magnetron sputtering. SPR tuning was achieved by different annealings, which affected the shape and size of the Au nanoparticles, and also the phase of the dielectric matrix. These changes promoted the variations on the optical properties. As shown by the modeling of the effective dielectric function of the TiO₂/Au in the SPR region, the variation of their optical absorption spectra correlates with morphological changes.

© 2010 Elsevier B.V. All rights reserved.

1. Introduction

The interest in composite materials containing metal nanoparticles (NPs) embedded in dielectric matrices is related to their potential application in a wide range of technological applications, such as colored coatings [1], solar cells [2], sensors [3,4], antibacterial [5] photocatalysis [6–8], and nonlinear optics [2,9,10]. TiO₂ is a transparent semiconductor material with a wide band gap $E_g = 3.2$ – 3.4 (eV) and high refractive index ($n = 2.5$ – 2.9) used for metal-dielectric composites designed for obtaining desired optical properties in the visible range.

The brilliant colors of composites containing noble metal inclusions are due to SPRs in the metallic phase [11]. Films with well-separated embedded metallic NPs with dimensions significantly smaller than the wavelength of the exciting light are characterized by a peak in the visible range of the absorption spectra. The band width, intensity, and position of the absorption maximum depend on the surrounding dielectric matrix, the size, distribution and especially on the shape of the NPs. This fact allows to tune the optical properties of the composite, (i) by changing the refractive index of the matrix (n_h) and (ii) by modifying the morphology and distribution of the metallic inclusions changing the aspect ratio of metallic NPs [12].

2. Experimental details

TiO₂/Au composite films were deposited on glass/quartz substrates, and *in-situ* Au doped by one step reactive magnetron sputtering process, at a constant temperature of 150 °C [13]. The deposited films were annealed in order to promote changes in the

morphology, distribution and structural features of *in-situ* grown gold NPs. The doping leads to an average Au volume fraction, f_{Au} , of about 12 at.% as determined by the Rutherford backscattering spectrometry (RBS).

The crystalline structure of as-grown and annealed films was investigated by X-ray diffraction (XRD), using a Philips PW 1710 diffractometer (Cu-K α radiation) operating in a Bragg-Brentano configuration. The XRD studies allowed to study the film structure concerning both the Au NPs and the TiO₂ matrix. Transmission electron microscopy (TEM) employing a Hitachy 800H apparatus was used to characterize the shape, size and spatial distribution of NPs. Color coordinates and absorption spectra were measured using a commercial MINOLTA CM-2600d and a UV-vis-NIR spectrophotometer (UV-3101) respectively [4,13].

3. Results and discussion

According to the RBS data, there were no measurable changes in the Au doping profiles across the 300 nm of the entire films' thickness during the annealing. The SPR-mediated color control has been achieved by means of annealing of TiO₂/Au composite films grown by reactive magnetron sputtering. Fig. 1 shows the color coordinates (L^* , a^* , b^*) and the change after annealing at different temperatures. Concerning the TiO₂ matrix, the XRD studies revealed that it is amorphous in as-grown and at low temperature annealed conditions. At 500 °C the TiO₂ dielectric matrix starts to crystallize in an anatase-type structure, transforming to rutile above 700 °C. Simultaneously, the Au atoms are organized in crystalline nanoparticles (revealing a fcc-type structure, with the (111) preferential growth orientation) [4,13].

Optical spectra, together with the corresponding morphological data, are depicted in Fig. 2. As it can be seen the SPR related absorption of light occurs only in the films annealed at 400 °C or higher

* Corresponding author.

E-mail address: marc.faro@fisica.uminho.pt (M. Torrell).

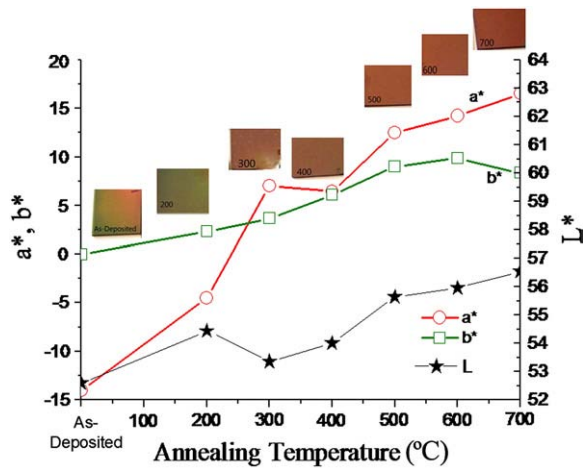


Fig. 1. Color coordinates (L^* , a^* , b^*) and the appearance of TiO_2/Au composite films annealed at different temperatures.

temperatures. The intensity of the resonance absorption increases with the annealing temperature and so does the NP size, as revealed by the TEM images of the same figure. At higher annealing temperatures the SPR band shifts to longer wavelengths and changes its shape. From the theoretical result obtained for a perfectly spherical metallic particle, often referred to as the Mie theory [14] the SPR condition is:

$$\epsilon_s + 2\epsilon_h = 0 \quad (1)$$

where $\epsilon_h = n_h^2$ is the dielectric constant of the host (matrix) and ϵ_s denotes the metal-dielectric function. In the simple Drude model,

$$\epsilon_s(\omega) = \epsilon_\infty \left[1 - \frac{\omega_p^2}{\omega(\omega + i\Gamma_p)} \right] \quad (2)$$

where ϵ_∞ is a constant, ω_p is the plasma frequency and Γ_p is a damping parameter. Assuming $\Gamma_p \ll \omega_p$, it follows from Eqs. (1) and (2) that the SPR frequency for a sphere is given by

$$\omega_{\text{SPR}} = \frac{\omega_p}{\sqrt{1 + 2\epsilon_h/\epsilon_\infty}} \quad (3)$$

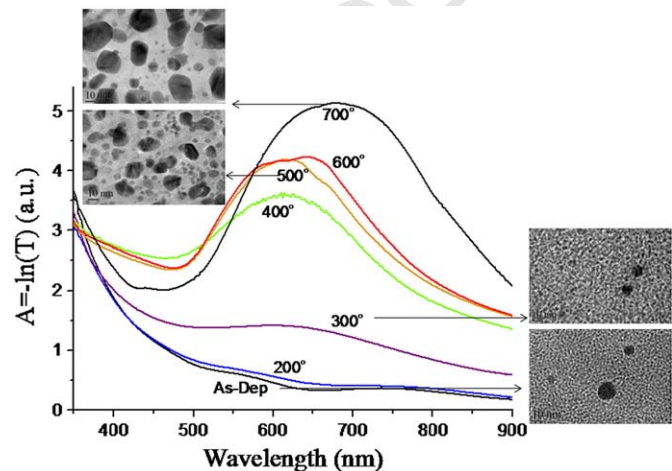


Fig. 2. Optical transmittance spectra (plotted in logarithmic scale) of a set of TiO_2/Au composite films annealed at different temperatures. TEM images of four representative films are also shown.

The width of a single SPR is determined mostly by the plasmon damping which depends on the NP size. For spherical Au NPs the following expression has been proposed [15].

$$\hbar\Gamma_p(R) = \hbar\Gamma_p(\text{bulk}) + g_s v_F / R = 0.0244 + 0.922g_s / R \quad [\text{eV}], \quad (4)$$

where v_F is the Fermi velocity, g_s is a geometrical factor of the order of unity and the NP radius R is in nanometers (For the geometrical factor, a value of $g_s \approx 0.7$ has been suggested) [16]. The intensity of the resonance is inversely proportional to Γ_p and directly proportional to the particle volume (R^3). Thus, the theory predicts that the intensity of the SPR band decreases and its broadening increases with the decrease of the NP size. It is experimentally demonstrated when samples annealed at 300 °C and 400 °C are compared (Fig. 2). However, for higher temperatures the absorption band becomes broader and its shape changes suggesting that perhaps there are more than one resonance involved.

The single SPR defined by Eqs. (1)–(3) is split if the particles are not spherical [17]. Axial-symmetric nanorods are supposed to produce two SPRs,

$$\omega'_{\text{SPR}} = \frac{\omega_p}{\sqrt{1 + (\eta_{\parallel}^{-1} - 1)\epsilon_h/\epsilon_\infty}}; \quad \omega''_{\text{SPR}} = \frac{\omega_p}{\sqrt{1 + (\eta_{\perp}^{-1} - 1)\epsilon_h/\epsilon_\infty}} \quad (5)$$

where η_{\parallel} and η_{\perp} are so called depolarization coefficients [18], which are some geometrical factors, non-negative numbers obeying the relation $\eta_{\parallel} + 2\eta_{\perp} = 1$. The first resonance takes place for electromagnetic wave polarized along the nanorod axis while the second one corresponds to the perpendicular polarization. If nanorods are embedded in a matrix in a random-orientation fashion, then one should expect to observe both SPRs. If we approximate nanorods by elongated (prolate) spheroids with eccentricity e , the depolarization coefficients are given by [18]:

$$\eta_{\parallel} = \frac{1-e^2}{e^3} \left(\frac{1}{2} \log \frac{1+e}{1-e} - e \right) \leq \frac{1}{3}; \quad \eta_{\perp} = \frac{1-\eta_{\parallel}}{2} \geq \frac{1}{3}. \quad (6)$$

Using these relations one can see that $\omega'_{\text{SPR}} < \omega_{\text{SPR}} < \omega''_{\text{SPR}}$. The two resonances corresponding to Eq. (4) merge into a single one determined by Eq. (3), when $\eta_{\parallel} = \eta_{\perp} = 1/3$ (spherical NPs).

Another effect clearly seen in Fig. 2 is the red shift of the absorption band. This is related to a change in the phase composition of the matrix. As already demonstrated, the transition temperature of the anatase-rutile TiO_2 has been reported on a wide range of temperatures, depending on the structure and morphology of the film growth process [19,20], and occurs typically between 700 and 800 °C for the studied samples, as it is reported in previous publications [13]. The two phases have different values of the refractive index, $n_{\text{anatase}} = 2.5$ and $n_{\text{rutile}} = 2.9$ at $\lambda = 550 \text{ nm}$ proposed [21]. As the annealing temperature was increased, the matrix became more crystalline, increasing the refractive index, but some amorphous TiO_2 phase remains. Anatase is the main crystalline phase until 700 °C, and at higher annealing temperatures the TiO_2 matrix is richer in rutile and the value of ϵ_h is even higher [4,13].

A model of the optical properties of the TiO_2/Au composite films was performed in order to quantify the arguments. The effective dielectric function of the composite material was calculated using the previously developed modified Maxwell-Garnett (MMG) formalism, which takes into account the dipole–dipole interaction between polarized particles [22,23]. As in the classical Maxwell-Garnett approach, the (complex) effective dielectric function (ϵ^*) of the composite is related to the particle's polarizability (α) through the equation:

$$\frac{\epsilon^* - \epsilon_h}{\epsilon^* + 2\epsilon_h} = \frac{4\pi}{3} N\alpha \quad (7)$$

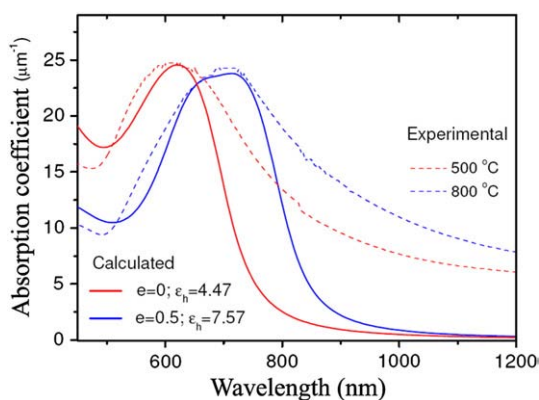


Fig. 3. Calculated and experimental optical absorption spectra of two TiO₂/Au films annealed at 500 and 800 °C, respectively (Au NPs 12 at %).

154 where N is the particle number per unit volume. However, in the
 155 MMG the polarizability is renormalized due to the dipole–dipole
 156 interactions between the particles and therefore this approach is valid
 157 for higher volume fractions of inclusions (see Refs [4,23] for further
 158 details). For the modeling purposes, the complex dielectric function of
 159 gold is used, where two extra contributions representing inter-band
 160 transitions have been included in addition to the Drude term (2) as
 161 proposed in the bibliography [24]. Dispersion of the refractive index of
 162 the TiO₂ matrix was taken into account according to the semi-
 163 empirical relations of Ref [25]. The value of $n_h(\lambda = 550 \text{ nm})$ was fitted
 164 by assuming a certain percentage of the amorphous and crystalline
 165 TiO₂ phases and voids.

166 Fig. 3 shows the modeling results of two representative spectra
 167 demonstrating the effects of the refractive index of the matrix (SPR band
 168 position) and NP's shape (band splitting). It is clearly seen that there are
 169 two separate resonances already for moderately elongated NPs ($e = 0.6$
 170 corresponds to the aspect ratio of approximately 1.25). These changes in
 171 the position and shape of the absorption band result in the variation of
 172 the film color coordinates (Fig. 1). The experimental spectra of Fig. 3 also
 173 show a long absorption tail extending to the near-infrared, not
 174 reproduced by the modelling. This absorption is attributed to more
 175 complex shapes gold inclusions. This assumption is supported by the
 176 TEM micrographs of Fig. 2 and it is known that metallic fractal clusters
 177 indeed can produce broad absorption spectra [26].

178 4. Conclusions

179 In conclusion, we have shown that the tuning of the Surface Plasmon
 180 Resonance is possible through the nanoscale control of the nanoparticle
 181 shape and the refractive index of the matrix, both being achieved by
 182 means of annealing treatments at appropriate temperatures.

183 Acknowledgements

184 This research is sponsored by FEDER funds through the program
 185 COMPETE-Programa Operacional Factores de Competitividade and by
 186

national funds through FCT-Fundação para a Ciência e a Tecnologia, 186
 under the project PTDC/CTM/70037/2006. 187

References 188

- [1] Takele H, Greve H, Pochstein C, Zaporozhchenko V, Faupel F. Plasmonic properties of Ag nanoclusters in various polymer matrices. *Nanotechnology* 2006;17:3499–505. 189
- [2] Walters G, Parkin IP. The incorporation of noble metal nanoparticles into host matrix films: synthesis, characterisation and applications. *J Mater Chem* 2009;19:574–90. 191
- [3] Hutter E, Fendler JH. Exploitation of localized Surface Plasmon Resonance. *Adv Mater* 2004;16:1685–706. 192
- [4] Torrell M, Machado P, Cunha L, Figueiredo NM, Oliveira JC, Louro C, et al. Development of new decorative coatings based on gold nanoparticles dispersed in an amorphous TiO₂ dielectric matrix. *Surf Coat Technol* 2010;204:1569–75. 193
- [5] Wang CM, Shutthanandan V, Zhang Y, Thevuthasan S, Thomas LE, Weber WJ, et al. Atomic level imaging of Au nanocluster dispersed in TiO₂ and SrTiO₃. *Nucl Instrum Methods Phys Res Sect B* 2006;242:380–2. 194
- [6] Pacholski C, Kornowski A, Weller H. Nanomaterials: site-specific photodeposition of silver on ZnO nanorods. *Angew. Chem Int Ed* 2004;43(36):4774–7. 195
- [7] Wu JJ, Tseng CH. Photocatalytic properties of nc-Au/ZnO nanorod composites. *Appl Catal B* 2006;66:51–7. 196
- [8] Li Y, Hu Y, Peng S, Lu G, Li S. Synthesis of CdS nanorods by an ethylenediamine assisted hydrothermal method for photocatalytic hydrogen evolution. *J Phys Chem C* 2009;113:9352–8. 197
- [9] Cho S, Lee S, Oh S, Park SJ, Kim WM, Cheong B, et al. Optical properties of Au nanocluster embedded dielectric films. *Thin Solid Films* 2000;377:97–102. 198
- [10] Hache F, Richard D, Flytzanis C, Kreibig K. The optical Kerr effect in small metal particles and metal colloids: the case of gold. *Appl Phys A* 1988;47:347–50. 199
- [11] Bohren CF, Huffman DR. Absorption and scattering of light by small particles. NY: Wiley; 1998. 200
- [12] Foss CA, Hornyak GL, Stockert JA, Martin CR. Template-synthesized nanoscopic gold particles: optical spectra and the effects of particle size and shape. *J Phys Chem B* 1994;98:2963–71. 201
- [13] M. Torrell, L. Cunha, A. Cavaleiro, E. Alves, N.P. Barradas, F. Vaz. Functional and optical properties of Au:TiO₂ nanocomposite films: the influence of thermal annealing. *Appl. Surf. Sci.* in press doi:10.1016/j.apsusc.2010.04.043. 202
- [14] Mie G. Beiträge zur Optik Trüber Medien, speziell Kolloidaler Metallösungen. *Ann Phys* 1908;25:377–452. 203
- [15] Ung T, Liz-Marzan LM, Mulvaney P. Optical properties of thin films of Au-SiO₂ particles. *J Phys Chem B* 2001;105:3441–52. 204
- [16] Baida H, Billaud P, Marhaba S, Christofilos D, Cottancin E, Crut A, et al. Quantitative determination of the size dependence of Surface Plasmon Resonance damping in single Ag@SiO₂ nanoparticles. *Nanoletters* 2009;9:3463–9. 205
- [17] Rodríguez-Fernández J, Novo C, Myroshnychenko V, Funston AM, Sánchez-Iglesias A, Pastoriza-Santos I, et al. Spectroscopy, imaging, and modeling of individual gold decahedra. *J Phys Chem C* 2009;113:18623–31. 206
- [18] Landau LD, Lifshitz EM. *Electrodynamics of Continuous Media*. Oxford: Pergamon; 1984. 207
- [19] Arroyo R, Córdoba G, Padilla J, Lara VH. Influence of manganese ions on the anatase-rutile phase transition of TiO₂ prepared by the sol-gel process. *Mater Lett* 2002;54:397–402. 208
- [20] Stech M, Reynders P, Rödel J. Constrained film sintering of nanocrystalline TiO₂. *J Am Ceram Soc* 2000;83(8):1889–96. 209
- [21] Song GB, Liang JK, Liu FS, Peng TJ, Rao GH. Preparation and phase transformation of anatase-rutile crystals in metal doped TiO₂/muscovite nanocomposites. *Thin Solid Films* 2005;491:110–6. 210
- [22] Vasilevskiy MI, Anda EV. Effective dielectric response of semiconductor composites. *Phys Rev B* 1996;54:5844–51. 211
- [23] Vasilevskiy MI. Effective dielectric response of composites containing uniaxial inclusions. *Phys Stat Sol B* 2000;219:197–204. 212
- [24] Etchegoin PG, Le Ru EC, Meyer M. An analytic model for the optical properties of gold. *J Chem Phys* 2006;125:164705–8. 213
- [25] Palik ED. *Handbook of optical constants of solids*, vol. 1. NY: Academic Press; 1985. 214
- [26] Shalaev VM. *Non-linear optics of random media*. Berlin: Springer; 2000. 215